J. Numer. Math., Vol. 0, No. 0, pp. 1–22 (2004)
© VSP 2004 *Prepared using* jnm.sty *[Version: 02.02.2002 v1.2]*

Analysis and simulation of a coupled hyperbolic/parabolic model problem

J.-P. Croisille,* A. Ern,† T. Lelièvre,† and J. Proft†‡

Received *Communicated by A. Quarteroni*

Abstract — We investigate a periodic, one-dimensional, linear, and degenerate advection-diffusion equation. The problem is hyperbolic in a subinterval and parabolic in the complement, and the boundary conditions only impose the periodicity of the advective-diffusive flux to ensure mass conservation. Following Gastaldi and Quarteroni (1989), a condition is added to select the "physically acceptable" solution as the limit of vanishing viscosity solutions, namely the continuity of the solution at the parabolic to hyperbolic interface. Using this condition, we establish the well-posedness of the Cauchy problem in the framework of the evolution linear semi-groups theory. We also discuss the regularity of the solution when the initial condition is too rough to be in the domain of the evolution operator. Then, we present reference solutions obtained using the additional interface condition. These solutions can be used to test the robustness of numerical schemes. Finally, we discuss results obtained with an upwind scheme, a finite volume box-scheme, and a local discontinuous Galerkin method. The three schemes (which do not enforce explicitly the additional interface condition) select automatically the physically acceptable solution, the two latter schemes being more accurate.

Keywords: Hyperbolic/parabolic, interface conditions, semi-group theory, discontinuous Galerkin, box-schemes, vanishing viscosity solution, porous media

1. INTRODUCTION

The main motivation for this work is to analyze the advection-diffusion of a scalar variable $u(t,x)$ in a medium having strong heterogeneities. Our aim is to address an evolution problem that changes spatially its mathematical character, namely hyperbolic in some parts of the domain and parabolic in the other parts. The model evolving $u(t,x)$ is the advection-diffusion equation

$$\partial_t u + \partial_x \mathscr{F}(x,u,\partial_x u) = f, \tag{1.1}$$

*Laboratoire de Mathématiques et Applications de Metz, UMR 7122, Université de Metz, Ile du Saulcy, F-57045 Metz cedex, France

†CERMICS, Ecole nationale des ponts et chaussées, 6/8 avenue Blaise Pascal, Champs sur Marne, F-77455 Marne-la-Vallée cedex 2, France

‡LAMA, CNRS UMR 8050, Université Marne-la-Vallée, Champs sur Marne, F-77454 Marne-la-Vallée cedex 2, France

This work was supported by CNRS and GdR MOMAS

with the flux

$$\mathscr{F}(x,u,\partial_x u) = \beta u - \alpha(x)\partial_x u. \tag{1.2}$$

The diffusion coefficient $\alpha(x)$ allows to switch between a purely advective equation ($\alpha(x) = 0$) and an advection-diffusion equation ($\alpha(x) > 0$). In applications, the variable $u(t,x)$ can mimic for instance a pollutant concentration in geological layers.

As a model problem, we investigate a 2-periodic setting in one space dimension. Let $\Omega = (0,2)$, $\Omega_P = (0,1)$, and $\Omega_H = (1,2)$. The advection velocity β is taken constant equal to 1 (the fluid flows in the sense of positive x); the diffusion coefficient is given by $\alpha(x) = \alpha_0 > 0$ for $x \in \Omega_P$ (the parabolic zone) and $\alpha(x) = 0$ for $x \in \Omega_H$ (the hyperbolic zone). We investigate the Cauchy problem

$$\begin{cases} \partial_t u + \partial_x \mathscr{F}(x,u,\partial_x u) = f & x \in \Omega,\ t > 0, \\ u(t=0,\cdot) = u_0 & x \in \Omega, \end{cases} \tag{1.3}$$

with advective-diffusive flux

$$\mathscr{F}(x,u,\partial_x u) = \begin{cases} u - \alpha_0\,\partial_x u & x \in \Omega_P, \\ u & x \in \Omega_H. \end{cases} \tag{1.4}$$

To specify boundary conditions, a minimal requirement for extending the solution to the whole real line by 2-periodicity is the continuity of the flux $\mathscr{F}$ at any interface where the diffusion coefficient is discontinuous. This property holds in particular at $1^-/1^+$ (parabolic to hyperbolic interface) and at $2^-/0^+$ (hyperbolic to parabolic interface), yielding

$$\begin{cases} u(1^-,t) - \alpha_0 \partial_x u(1^-,t) = u(1^+,t), \\ u(0^+,t) - \alpha_0 \partial_x u(0^+,t) = u(2^-,t). \end{cases} \tag{1.5}$$

The continuity of the flux is physically important since it expresses mass conservation. In contrast, no continuity conditions are imposed a priori on the solution at the interfaces. The goal of this paper is twofold. First, to present a mathematical setting in which (1.3)–(1.4)–(1.5) is well-posed. Second, to display reference solutions computed for various data sets (initial condition and diffusion coefficient) in order to provide a benchmark test suite. The two main difficulties to be tackled numerically are to capture the travelling singularities of the solution and to preserve high-accuracy for long time, i.e., after the initial condition has crossed the domain Ω several times.

Concerning the mathematical setting, it is important to observe that Problem (1.3)–(1.4)–(1.5) is ill-posed in the sense that it admits many solutions. To illustrate this point, consider the case of a null initial condition, $u_0 = 0$, and a null source term, $f = 0$. Consider any smooth function of time $\varphi : \mathbb{R}^+ \to \mathbb{R}$ such that $\varphi^{(n)}(0) = 0$ for all $n \geqslant 0$ (for example $\varphi(t) = a\exp(-b/t)$ with two constants a and $b > 0$). Impose the flux at $x = 1$ by setting $\mathscr{F}(t,1) = \varphi(t)$. Integrating along characteristics in Ω_H shows that the flux at $x = 2$ is $\mathscr{F}(t,2) = \varphi(t-1)1_{\{t \geqslant 1\}}$ (1_ω denotes

the characteristic function of the set ω). Consider the following parabolic problem on $(0,1)$ with Robin boundary conditions:

$$\begin{cases} \partial_t u + \partial_x u - \alpha_0 \partial_{xx} u = 0 & (t,x) \in (0,\infty) \times (0,1), \\ \left(u - \alpha_0 \partial_x u\right)(t,1) = \varphi(t), & t \in [0,\infty), \\ \left(u - \alpha_0 \partial_x u\right)(t,0) = \varphi(t-1) 1_{\{t \geqslant 1\}}, & t \in [0,\infty), \\ u(0,x) = 0, & x \in (0,1). \end{cases} \tag{1.6}$$

This problem admits a smooth solution, and from this solution it is straightforward to build a nonzero smooth solution to (1.3)–(1.4)–(1.5) with data $u_0 = 0$ and $f = 0$. Thus, an additional condition has to be specified to recover uniqueness, i.e., to select the unique "physically acceptable" solution. This difficulty has been analyzed in [9] for one-dimensional coupled parabolic/hyperbolic problems using vanishing viscosity techniques. It results from this study that the physically acceptable solution is continuous at any parabolic to hyperbolic interface whereas no continuity condition holds a priori at the other interfaces. In Section 2, we make clear that this additional condition is indeed needed to derive an existence and uniqueness result in the framework of the evolution linear semi-groups theory [2,12]. In particular, we prove that the evolution operator associated with (1.3) is maximal and monotone provided its domain is restricted to those functions that are continuous at the parabolic to hyperbolic interface. We also discuss the regularity of the solutions to (1.3)–(1.4)–(1.5) when the initial condition is too rough to be in the domain of the evolution operator.

Concerning the numerical results, we stress that a robust scheme should find "automatically" the physically acceptable solution, i.e., the continuity of the solution at the parabolic to hyperbolic interface should not be explicitly enforced by the scheme. To assess the schemes, reference solutions are computed for various sets of data using the problem-specific scheme described in Section 3. In each case, we present solution profiles at different times and various time-dependent functionals of the solution allowing to characterize the properties of the schemes to be tested. Of particular interest are the total energy and the value of the jump at the interface $2^-/0^+$. In Section 4, these reference results are used to assess on relatively coarse meshes the robustness and accuracy of various schemes: an upwind scheme, a box-scheme introduced in [7], and a locally discontinuous Galerkin method derived in [4].

2. MATHEMATICAL ANALYSIS

The goal of this section is twofold. First, to stress the importance of the continuity of the solution at the parabolic to hyperbolic interface in the framework of the evolution linear semi-groups theory. Second, to discuss the regularity of the solutions to the evolution problem when the initial condition is too rough to be in the domain of the evolution operator.

2.1. Evolution linear semi-groups theory

Without loss of generality, we assume in this section that $\alpha_0 = 1$. For simplicity, the flux given by (1.4) is denoted by $\mathscr{F}(u)$ instead of $\mathscr{F}(x,u,\partial_x u)$. For a smooth function v in $\Omega_P \cup \Omega_H$, we introduce the jumps $[v(1)] = v(1^+) - v(1^-)$ and $[v(2)] = v(0^+) - v(2^-)$. For functions only depending on the space variable, distributional derivatives are denoted by a subscript x. For an open set $E \subset \Omega$, the $L^2(E)$-inner product is denoted by $(\cdot,\cdot)_E$. Let $\mathscr{P}(\Omega)$ be the space of 2-periodic functions in $\mathscr{C}^\infty(\overline{\Omega})$ and let $H^1_{per}(\Omega)$ be the closure of $\mathscr{P}(\Omega)$ for the H^1-norm. Let

$$V = \{\, v \in H^2(\Omega_P) \cap H^1(\Omega_H),\ [\mathscr{F}(v)(1)] = [\mathscr{F}(v)(2)] = [v(1)] = 0 \,\}, \tag{2.1}$$

and consider the operator $A : D(A) \equiv V \to L^2(\Omega)$ defined by

$$Av = (\mathscr{F}(v))_x. \tag{2.2}$$

Theorem 2.1. *The operator $A : V \to L^2(\Omega)$ is the infinitesimal generator of a continuous semi-group of contractions $T(t) : L^2(\Omega) \to L^2(\Omega)$, $0 \leqslant t < \infty$.*

Proof. We use the Lumer–Phillips criterion [12, p. 14], i.e., we establish that A is monotone and maximal; see Lemmas 2.1 and 2.2 below. □

Corollary 2.1. For all $u_0 \in D(A)$ and $f \in C^1([0,\infty[;L^2(\Omega))$, the evolution problem

$$\begin{cases} \frac{\mathrm{d}u}{\mathrm{d}t} + Au = f \quad \forall t \in [0,\infty[, \\ u(0) = u_0, \end{cases} \tag{2.3}$$

admits a unique strong solution $u \in C^1([0,\infty);L^2(\Omega)) \cap C^0([0,\infty);D(A))$. This solution satisfies the a priori estimates

$$\|u(t)\|_\Omega \leqslant \|u_0\|_\Omega \quad \text{and} \quad \|\tfrac{\mathrm{d}u}{\mathrm{d}t}\|_\Omega \leqslant \|Au_0\|_\Omega, \quad \forall t \in [0,\infty[. \tag{2.4}$$

Proof. See, e.g., [12, p. 102]. □

Lemma 2.1. *The operator A is monotone:*

$$\forall v \in D(A), \quad (v,Av)_\Omega \geqslant 0. \tag{2.5}$$

Proof. Let $v \in D(A)$. Using integration by parts and the continuity of the flux at $1^-/1^+$ and $2^-/0^+$ yields

$$\begin{aligned} (v,Av)_\Omega &= \textstyle\int_0^1 v(\mathscr{F}(v))_x\,\mathrm{d}x + \int_1^2 v(\mathscr{F}(v))_x\,\mathrm{d}x \\ &= -\textstyle\int_0^2 v_x \mathscr{F}(v)\,\mathrm{d}x - \mathscr{F}(v)(1)[v(1)] - \mathscr{F}(v)(2)[v(2)] \\ &= \textstyle\int_0^1 (v_x)^2\,\mathrm{d}x + \frac{1}{2}[v^2(1)] + \frac{1}{2}[v^2(2)] - v(1^+)[v(1)] - v(2^-)[v(2)] \\ &= \textstyle\int_0^1 (v_x)^2\,\mathrm{d}x + \frac{1}{2}[v(2)]^2 - \frac{1}{2}[v(1)]^2. \end{aligned}$$

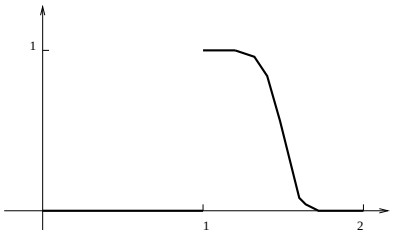

Figure 1. A suitable function ψ for the proof of Lemma 2.2.

Since $v \in D(A)$, $[v(1)] = 0$ implying $(v, Av)_\Omega \geqslant 0$. □

Lemma 2.2. *The operator A is maximal:*

$$\forall g \in L^2(\Omega), \quad \exists u \in D(A) \quad s.t. \quad u + Au = g. \tag{2.6}$$

Proof. Let $g \in L^2(\Omega)$. The solution u in (2.6) is constructed as the vanishing viscosity limit of a sequence of solutions to a regularized problem. Henceforth, c denotes a generic constant that may depend on g but not on the vanishing viscosity ε and whose value may change at each occurrence.
Step 1. Let $\varepsilon > 0$. For $v \in H^1_{per}(\Omega)$, define $\mathscr{F}^\varepsilon(v) = v - v_x$ in Ω_P, $\mathscr{F}^\varepsilon(v) = v - \varepsilon v_x$ in Ω_H, and $A^\varepsilon v = (\mathscr{F}^\varepsilon(v))_x$. Clearly, the problem

$$(u^\varepsilon, \varphi)_\Omega + (\mathscr{F}^\varepsilon(u^\varepsilon), \varphi_x)_\Omega = (g, \varphi)_\Omega, \qquad \forall \varphi \in H^1_{per}(\Omega), \tag{2.7}$$

admits a unique solution $u^\varepsilon \in H^1_{per}(\Omega)$. Note that (2.7) implies $u^\varepsilon + A^\varepsilon u^\varepsilon = g$ in $L^2(\Omega)$ and $[\mathscr{F}^\varepsilon(u^\varepsilon)(2)] = 0$. Testing (2.7) by u^ε yields the a priori estimates

$$\|u^\varepsilon\|_{L^2(\Omega)} \leqslant c, \qquad \|u^\varepsilon\|_{H^1(\Omega_P)} \leqslant c, \qquad \sqrt{\varepsilon}\|u^\varepsilon\|_{H^1(\Omega_H)} \leqslant c. \tag{2.8}$$

This implies $\|\mathscr{F}^\varepsilon(u^\varepsilon)\|_{L^2(\Omega)} \leqslant c$. Moreover, since $(\mathscr{F}^\varepsilon(u^\varepsilon))_x = g - u^\varepsilon$, it is clear that $\|(\mathscr{F}^\varepsilon(u^\varepsilon))_x\|_{L^2(\Omega)} \leqslant c$; hence,

$$\|\mathscr{F}^\varepsilon(u^\varepsilon)\|_{H^1_{per}(\Omega)} \leqslant c. \tag{2.9}$$

The last important estimate consists of controlling the H^1-norm of u^ε in the neighborhood of $x = 1$ uniformly in ε. Let $0 < \alpha < 1$. There exists a positive function ψ which is zero on $(0,1)$ and on a neighborhood of 2, equal to one on the interval $[1, 1+\alpha]$, smooth over $(1,2)$, and non-increasing on the same interval; see Figure 1. Testing (2.7) by $u^\varepsilon_x \psi$ and integrating over $(1,2)$ yields

$$\int_1^2 u^\varepsilon u^\varepsilon_x \psi \, dx + \int_1^2 (u^\varepsilon_x)^2 \psi \, dx - \varepsilon \int_1^2 u^\varepsilon_{xx} u^\varepsilon_x \psi \, dx = \int_1^2 g u^\varepsilon_x \psi \, dx, \tag{2.10}$$

noticing that all the integrals are well-defined. Integration by parts of the third integral in the left-hand side leads to

$$-\int_1^2 u_{xx}^\varepsilon u_x^\varepsilon \psi \,\mathrm{d}x = \frac{1}{2}\int_1^2 (u_x^\varepsilon)^2 \psi_x \,\mathrm{d}x + \frac{1}{2}(u_x^\varepsilon)^2(1). \tag{2.11}$$

Hence,

$$\int_1^2 (u_x^\varepsilon)^2 \psi \,\mathrm{d}x \leqslant -\int_1^2 u^\varepsilon u_x^\varepsilon \psi \,\mathrm{d}x + \int_1^2 g u_x^\varepsilon \psi \,\mathrm{d}x + \frac{\varepsilon}{2}\int_1^2 (u_x^\varepsilon)^2 |\psi_x| \,\mathrm{d}x. \tag{2.12}$$

Owing to the inequality $ab \leqslant \gamma a^2 + \frac{1}{4\gamma} b^2$ valid for all $\gamma > 0$, there exists c such that

$$c\int_1^2 (u_x^\varepsilon)^2 \psi \,\mathrm{d}x \leqslant \int_1^2 (u^\varepsilon)^2 \psi \,\mathrm{d}x + \int_1^2 g^2 \psi \,\mathrm{d}x + \frac{\varepsilon}{2}\int_1^2 (u_x^\varepsilon)^2 |\psi_x| \,\mathrm{d}x, \tag{2.13}$$

which combined with the first and third a priori estimates in (2.8) yields

$$\|u^\varepsilon\|_{H^1(1-\alpha,1+\alpha)} \leqslant c. \tag{2.14}$$

The continuity condition $[u(1)] = 0$ in $D(A)$ is rooted in this estimate.
Step 2. Owing to (2.8) and (2.9), there is a subsequence u^{ε_n} of u^ε such that $u^{\varepsilon_n} \rightharpoonup u$ in $L^2(\Omega)$, $u^{\varepsilon_n} \rightharpoonup u$ in $H^1(\Omega_P)$, and $\mathscr{F}^{\varepsilon_n}(u^{\varepsilon_n}) \rightharpoonup \overline{\mathscr{F}}$ in $H^1_{per}(\Omega)$. Passing to the limit in (2.7) implies that u satisfies $u + Au = g$ in $\mathscr{D}'(\Omega_P)$ and $\mathscr{D}'(\Omega_H)$. Moreover, it is clear that $\overline{\mathscr{F}} = u - u_x$ in Ω_P. In Ω_H, $u^{\varepsilon_n} - \mathscr{F}^{\varepsilon_n}(u^{\varepsilon_n}) = \varepsilon_n u_x^{\varepsilon_n}$; the left-hand side converges to $u - \overline{\mathscr{F}}$ in $\mathscr{D}'(\Omega_H)$ and the right-hand side converges to 0 in $L^2(\Omega_H)$ owing to the third estimate in (2.8). Therefore, $\overline{\mathscr{F}} = u$ in Ω_H. Hence, $\overline{\mathscr{F}} = \mathscr{F}(u)$ in Ω with $\mathscr{F}(u)$ defined by (1.4). Since $\overline{\mathscr{F}}$ is in $H^1_{per}(\Omega)$, $[\mathscr{F}(u)(1)] = [\mathscr{F}(u)(2)] = 0$. Finally, estimate (2.14) implies that (up to the extraction of a new subsequence) the limit u is continuous in a neighborhood of 1. Hence, $u \in D(A)$ and $u + Au = g$ in $L^2(\Omega)$, which concludes the proof. □

Remark 2.1. Clearly, the solution u to (2.6) is unique since $u + Au = 0$ and $u \in D(A)$ implies $\|u\|^2_{L^2(\Omega)} = 0$ owing to the monotonicity of A. Therefore, the operator $(I + A)$ is bijective from $D(A)$ into $L^2(\Omega)$. Let $B : D(B) \equiv W \to L^2(\Omega)$ be the extension of A to the space W defined as in (2.1) by omitting the interface condition $[v(1)] = 0$. Then, one readily verifies that the equation $u + Bu = 0$ admits infinitely many solutions in $D(B)$, i.e., the operator $(I + B)$ is not injective from $D(B)$ to $L^2(\Omega)$.

Remark 2.2. Since A is monotone and maximal and since $L^2(\Omega)$ is reflexive, its domain $D(A)$ is dense in $L^2(\Omega)$; see, e.g., [12, p. 16]. Moreover, for all $\lambda > 0$, the operator $(I + \lambda A)$ is bijective from $D(A)$ to $L^2(\Omega)$, $(I + \lambda A)^{-1}$ is bounded in $L^2(\Omega)$, and $\|(I + \lambda A)^{-1}\|_{\mathscr{L}(L^2(\Omega))} \leqslant 1$; see, e.g., [1].

Remark 2.3. The argument in the proof of Lemma 2.2 cannot be used to prove that the H^1-norm of u^ε is uniformly bounded on a left neighborhood of 2 with the function $\varphi(x) = \psi(3-x)$. Indeed, after integration by parts, one obtains

$$-\int_1^2 u^\varepsilon_{xx}\, u^\varepsilon\, \varphi \,\mathrm{d}x = \frac{1}{2}\int_1^2 (u^\varepsilon_x)^2\, \varphi_x \,\mathrm{d}x - \frac{1}{2}(u^\varepsilon_x)^2(2), \tag{2.15}$$

and one cannot conclude owing to the sign of the last term in the right-hand side.

Remark 2.4. Let u^ε be the time-dependent solution of the evolution problem in which a small diffusion coefficient ε is added in Ω. Then, if $u_0 \in H^2(\Omega) \cap D(A)$, using the same techniques as in the proof of Lemma 2.2, one can show that u^ε converges to the semi-group solution $T(t)u_0$. This justifies the fact that the continuity condition for the solution at $x = 1$ can be captured by a vanishing viscosity technique.

2.2. Rough initial data

In this section we construct weak and strong solutions to (1.3)–(1.4) when u_0 is too rough to be in the domain of A, e.g., $u_0 \in L^2(\Omega)$ only. We limit ourselves to the homogeneous case, $f \equiv 0$. Our main result is that under some assumptions, once the initial condition has crossed Ω_H, i.e., at time $t > 1$, the solution is smooth enough to be in $D(A)$. This is a consequence of the smoothing effect of the evolution operator in Ω_P. Let $Y = L^\infty((0,\infty);L^2(\Omega_P)) \cap L^2((0,\infty);H^1(\Omega_P)) \cap L^2((0,\infty);L^2(\Omega_H))$. A weak solution to (1.3)–(1.4) in Y is constructed as follows.

First, seek $u_P \in L^\infty((0,\infty);L^2(\Omega_P)) \cap L^2((0,\infty);H^1(\Omega_P))$ such that $u_P(t=0,\cdot) = u_{0|\Omega_P}$ and, for all $\varphi \in H^1(\Omega_P)$ and a.e. in t,

$$(\partial_t u_P, \varphi)_{\Omega_P} - (u_P - \partial_x u_P, \partial_x \varphi)_{\Omega_P} + u_P(t,1)\varphi(1) = \omega(t)\varphi(0), \tag{2.16}$$

where

$$\omega(t) = u_0(2-t)1_{\{t<1\}} + u_P(t-1,1)1_{\{t>1\}}. \tag{2.17}$$

Standard energy estimates show that Problem (2.16) is well-posed. The unique solution u_P solves the evolution equation (1.3)–(1.4) in $\mathscr{D}'((0,\infty)\times\Omega_P)$ and satisfies weakly the Robin condition $u_P(t,0) - \partial_x u_P(t,0) = \omega(t)$ and the homogeneous Neumann condition $\partial_x u_P(t,1) = 0$.

Second, use the value $u_P(t,1)$ to feed the advection equation

$$\partial_t u_H + \partial_x u_H = 0, \quad \text{in } \mathscr{D}'((0,\infty)\times\Omega_H). \tag{2.18}$$

Finally, set $u_{|\Omega_P} = u_P$ and $u_{|\Omega_H} = u_H$. Then, $u \in Y$, u is a weak solution of (1.3)–(1.4) in $\mathscr{D}'((0,\infty)\times\Omega)$, $u(t,\cdot)$ is continuous at 1 for $t > 0$, and the flux $\mathscr{F}(u)$ satisfies weakly the interface conditions. The condition at $2^-/0^+$ results from the Robin condition and the fact that $u_H(t,2) = u_P(t-1,1)$; the condition at $1^-/1^+$ results from

the homogeneous Neumann condition and the fact that the solution u is continuous at 1.

To obtain stronger regularity results on the solution $u \in Y$ constructed above, we slightly restrict the class of initial conditions. The proofs below are only sketched since they use well-known energy techniques; see, e.g., [11,13].

Lemma 2.3. *Let $u_0 \in H^1(\Omega) \cap H^2(\Omega_P)$. Then, the solution $u \in Y$ constructed above is in $C^1((0,\infty);L^2(\Omega)) \cap C^0((0,\infty);D(A))$, i.e., it coincides with the semi-group solution for $t > 0$.*

Proof. Since $u_0 \in H^1(\Omega_H)$, $\omega \in H^1(0,1)$ in time. Testing the time-derivative of (2.16) by $\partial_t u_P$ (this can be justified rigorously by first working in finite dimension and then passing to the limit; see, e.g., [11, p. 80]) yields

$$\frac{1}{2}\frac{\mathrm{d}}{\mathrm{d}t}\|\partial_t u_P\|_{\Omega_P}^2 + \|\partial_{xt} u_P\|_{\Omega_P}^2 - (\partial_t u_P, \partial_{xt} u_P)_{\Omega_P} + (\partial_t u_P(t,1))^2 = \omega'(t)\partial_t u_P(t,0). \tag{2.19}$$

Using Young's inequality to hide the third term in the left-hand side and the right-hand side, dropping the fourth term, and then using a Gronwall's Lemma, we infer, for any time $0 < T < 1$,

$$\|\partial_t u_P(T,\cdot)\|_{\Omega_P}^2 + \int_0^T \|\partial_{xt} u_P\|_{\Omega_P}^2 \,\mathrm{d}t \leqslant c(\|u_0\|_{H^1(\Omega_H)}^2 + \|\partial_t u_P(0,\cdot)\|_{\Omega_P}^2). \tag{2.20}$$

The last term in the right-hand side is controlled since $u_0 \in H^2(\Omega_P)$. Hence, $\partial_t u_P \in L^\infty((0,\infty);L^2(\Omega_P)) \cap L^2((0,\infty);H^1(\Omega_P))$ implying that $u_P(t,x=1)$ is H^1 in time. Since u_0 is assumed to be continuous at $x = 1$, $u_H(t,\cdot) \in H^1(\Omega_H)$. Therefore, $u(t)$ is in $D(A)$ for $t > 0$; hence, for $t > 0$, u coincides with the solution given by the evolution semi-groups theory. □

Proposition 2.1. *Let $u_0 \in L^2(\Omega_P) \cap H^1(\Omega_H)$. Then, the solution $u \in Y$ constructed above is in $C^1((1,\infty);L^2(\Omega)) \cap C^0((1,\infty);D(A))$, i.e., it coincides with the semi-group solution for $t > 1$.*

Proof. Since $u_P \in L^2((0,\infty);H^1(\Omega_P))$, there is an arbitrarily small time $\varepsilon_1 > 0$ such that $u_P(\varepsilon_1,\cdot) \in H^1(\Omega_P)$. Testing (2.16) by $\partial_t u_P$ (this can be justified rigorously; see, e.g., [13, p. 370]) and proceeding as before, one can prove that, for $\varepsilon_1 < T < 1$,

$$\|u_P(T,\cdot)\|_{H^1(\Omega_P)}^2 + \int_{\varepsilon_1}^T \|\partial_t u_P(t,\cdot)\|_{\Omega_P}^2 \,\mathrm{d}t \leqslant c(\|u_P(\varepsilon_1,\cdot)\|_{H^1(\Omega_P)}^2 + \|u_0\|_{H^1(\Omega_H)}^2). \tag{2.21}$$

Hence, $u_P \in L^\infty((\varepsilon_1,1);H^1(\Omega_P)) \cap H^1((\varepsilon_1,1);L^2(\Omega_P))$. As a result, for an arbitrarily small time $\varepsilon_2 > \varepsilon_1$, $u(\varepsilon_2,\cdot) \in H^1(\Omega) \cap H^2(\Omega_P)$. Using $u(\varepsilon_2,\cdot)$ as an initial condition and reasoning as in the proof of Lemma 2.3 yields $\partial_t u_P \in L^\infty((\varepsilon_2,1);L^2(\Omega_P)) \cap L^2((\varepsilon_2,1);H^1(\Omega_P))$. As a result, $u(\cdot,x=1)$ is continuous in time for $t \in (\varepsilon_2,1)$ and

hence for $t \in (0,1)$ since ε_2 is arbitrary. Moreover,

$$u(t,\cdot) \in H^2(\Omega_P) \cap H^1(0,1+t) \cap H^1(1+t,2), \quad 0 < t < 1. \tag{2.22}$$

This, in turn, implies that for $0 < t < 1$, the flux is continuous both at $1^-/1^+$ and at $2^-/0^+$. Hence, $u(t=1,\cdot) \in H^1(\Omega) \cap H^2(\Omega_P)$ and for $t > 1$, u coincides with the semi-group solution. □

Remark 2.5. Assume that u_0 is continuous at $x = 1$ and is piecewise H^1 in Ω_H, i.e., there exists a finite sequence $1 < x_1 < \cdots < x_N < 2$ such that $u_{|\Omega_H} \in H^1(1,x_1) \cup \cdots \cup H^1(x_N,1)$. Then, the solution $u \in Y$ constructed above is a strong solution for $t > t_* = 2 - x_1$, i.e., after the last singularity in u_0 has crossed Ω_H. See test cases 2 and 3 in Section 3.2.

Remark 2.6. In view of the results of Sections 2.1 and 2.2, the question which is left open is to know whether the semi-group solution $u(t) = T(t)u_0$, $u_0 \in L^2(\Omega)$, coincides with the solution $u \in Y$ constructed above during the time interval $(0,1)$.

3. REFERENCE SOLUTIONS

This section presents reference solutions for the evolution problem (1.3)–(1.4)–(1.5) for various sets of data. Reference solutions are obtained computationally using a problem-specific scheme with built-in interface condition.

3.1. A scheme with built-in interface condition

The idea is to use continuous piecewise-linear finite elements to discretize the advection-diffusion equation in Ω_P and to use exact integration along characteristics to solve the purely advective equation in Ω_H. The scheme is able to build a solution by capturing the flux $\mathscr{F}(u)(1)$ according to a prescribed criterion (zero jump of the solution at a certain point or minimizing any global quantity as the energy). In the context of vanishing viscosity solutions, this criterion is obviously the zero-jump condition at $1^-/1^+$. To simplify the presentation, we assume that the source term f is identically zero on Ω. The scheme can be easily extended to the general case by appropriate time-integration along characteristics.

Let u solve (1.3)–(1.4)–(1.5) and let $\varphi_1(t) = \mathscr{F}(u)(t,1)$ be the flux at $x = 1$. Since $u(t,1^+) = \varphi_1(t)$, the purely advective equation can be integrated exactly on Ω_H to yield the flux at $x = 2$,

$$\varphi_2(t) = u(t,2^-) = u_0(2-t)1_{\{t \leqslant 1\}} + \varphi_1(t-1)1_{\{t \geqslant 1\}}. \tag{3.1}$$

Owing to the periodicity of the flux, $u_{|\Omega_P}$ satisfies the following evolution problem

with Robin boundary conditions:

$$\begin{cases} \partial_t u + \partial_x u - \alpha_0 \partial_{xx} u = 0 & (t,x) \in [0,\infty) \times (0,1), \\ \left(u - \alpha_0 \partial_x u\right)(t,1) = \varphi_1(t) & t \in [0,\infty), \\ \left(u - \alpha_0 \partial_x u\right)(t,0) = \varphi_2(t) & t \in [0,\infty), \\ u(0,x) = u_0 & x \in (0,1). \end{cases} \tag{3.2}$$

Let $\mathscr{M}_P = \cup_{j=1}^{N_P} [x_j, x_{j+1}]$ be a mesh of Ω_P and let V_P be the space spanned by continuous piecewise-linear functions on this mesh. The finite element approximation to (3.2) consists of seeking $u_h \in C^1([0,\infty[;V_P)$ such that, for all $v_h \in V_P$ and $t \geqslant 0$,

$$\tfrac{\mathrm{d}}{\mathrm{d}t}(u_h, v_h)_{\Omega_P} - (\mathscr{F}(u_h), v_{h,x})_{\Omega_P} + \varphi_1(t)\, v_h(1) - \varphi_2(t)\, v_h(0) = 0. \tag{3.3}$$

Equation (3.3) is discretized in time by an implicit Euler scheme, yielding

$$\tfrac{1}{\delta t}(u_h^{n+1} - u_h^n, v_h)_{\Omega_P} - (\mathscr{F}(u_h^{n+1}), v_{h,x})_{\Omega_P} + \varphi\, v_h(1) - \varphi_2(t^{n+1})\, v_h(0) = 0, \tag{3.4}$$

where $\delta t \leqslant 1$ is the time step and φ is the yet unknown flux $\varphi_1(t^{n+1})$. Owing to (3.1), the flux $\varphi_2(t^{n+1})$ can be evaluated explicitly using known values of the initial condition and of the flux $\varphi_1(t)$ at previous time steps. The solution u_h^{n+1} of (3.4) is an affine function of φ. Evaluating it with two trial values for φ, it is possible to determine the value of φ for which $u_h^{n+1}(1) = \varphi$, i.e., the value of the flux for which the zero-jump condition is satisfied.

3.2. Test cases

We consider the following test cases:

- Case 1: $\alpha_0 = 0.05$ and $u_0(x) = 16x^2(1-x)^2 1_{\{x\in[0;1]\}}$.
- Case 2: $\alpha_0 = 0.05$ and $u_0(x) = 1_{\{x\in[1.;1.25]\}}$.
- Case 3: $\alpha_0 = 1$ and $u_0(x) = 1_{\{x\in[1.;1.25]\}}$.

Note that u_0 is in the domain $D(A)$ defined in Section 2.1 in case 1 only. Simulations are performed on the time interval $(0,5)$ using 10^6 time steps and a uniform mesh of $(0,1)$ with cell spacing $h = 10^{-3}$. Figures 2–4 present the following results:

- The $L^\infty(\Omega)$-norm of u and the energy $\mathscr{E}(t)$ defined as

$$\mathscr{E}(t) = \frac{1}{2}\int_0^2 u(t,x)^2\,\mathrm{d}x + \alpha_0 \int_0^t \left(\int_0^1 (\partial_x u(t,x))^2\,\mathrm{d}x\right)\mathrm{d}t, \tag{3.5}$$

  and normalized by $\mathscr{E}(0)$; both quantities are displayed as a function of time. Owing to Lemma 2.1, the energy decreases in time (since $f = 0$).

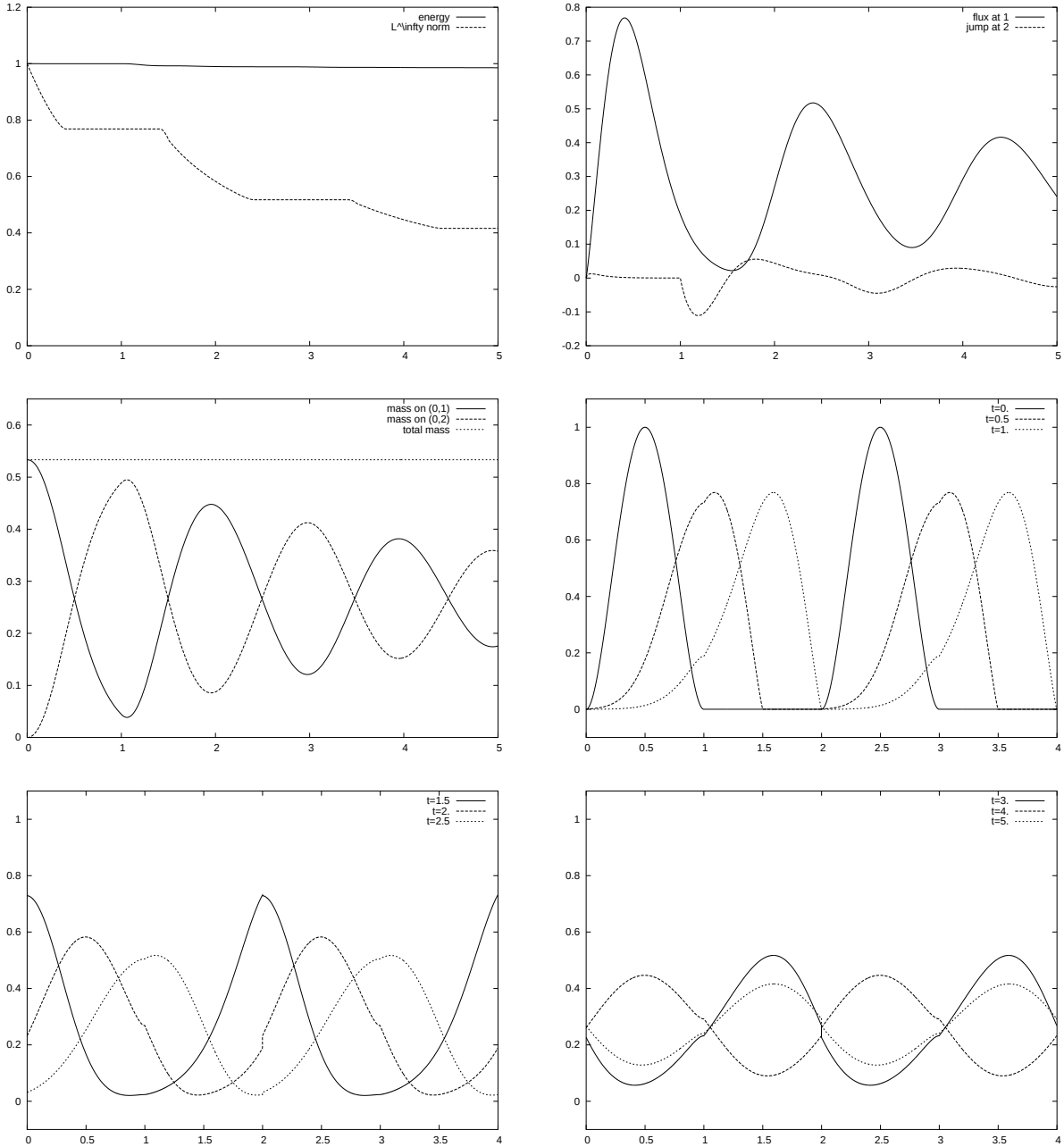

Figure 2. Reference solution for case 1: $\alpha = 0.05$ and $u_0(x) = 16x^2(1-x)^2 1_{\{x\in[0;1]\}}$.

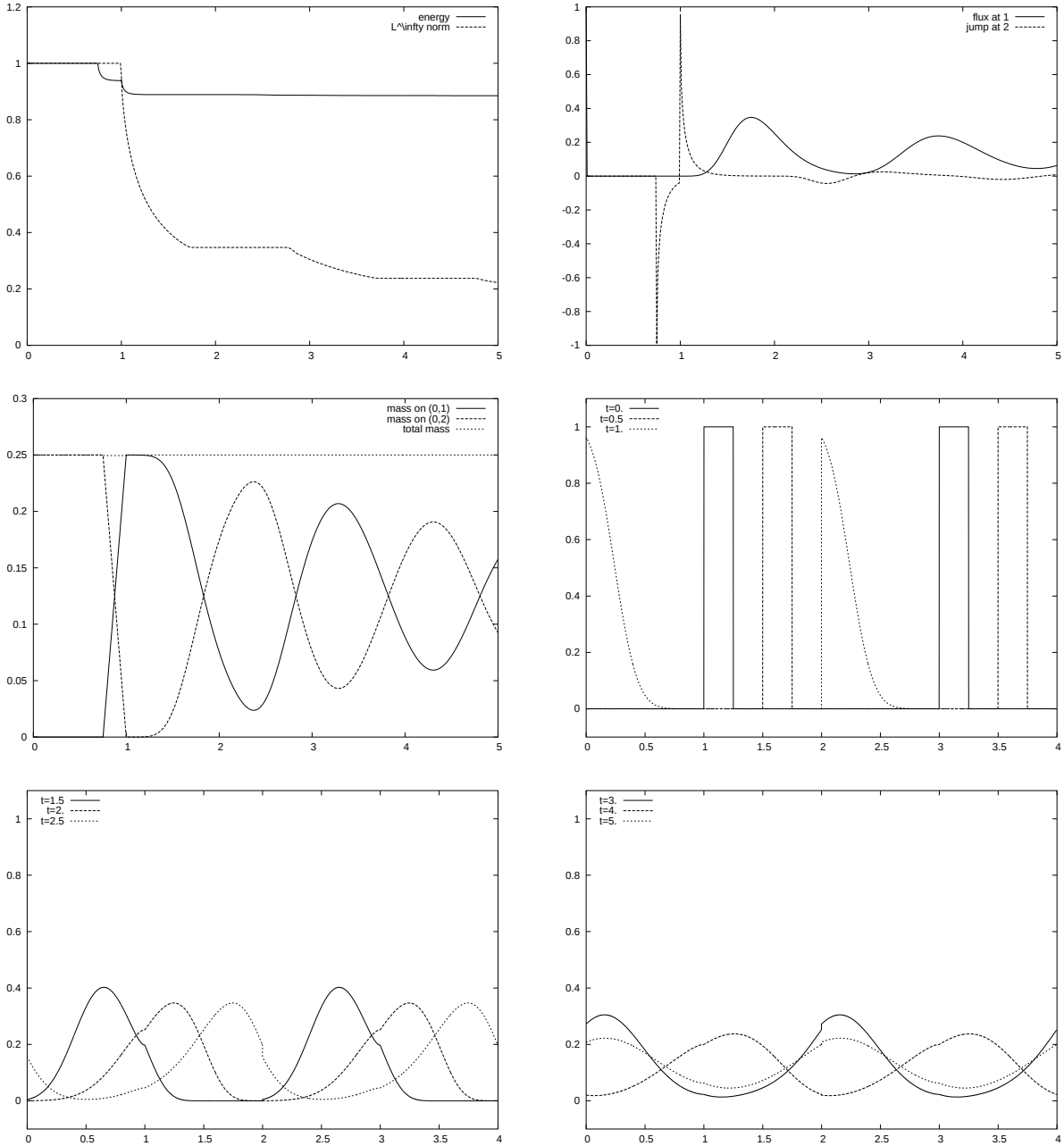

Figure 3. Reference solution for case 2: $\alpha = 0.05$ and $u_0(x) = 1_{\{x\in[1.;1.25]\}}$.

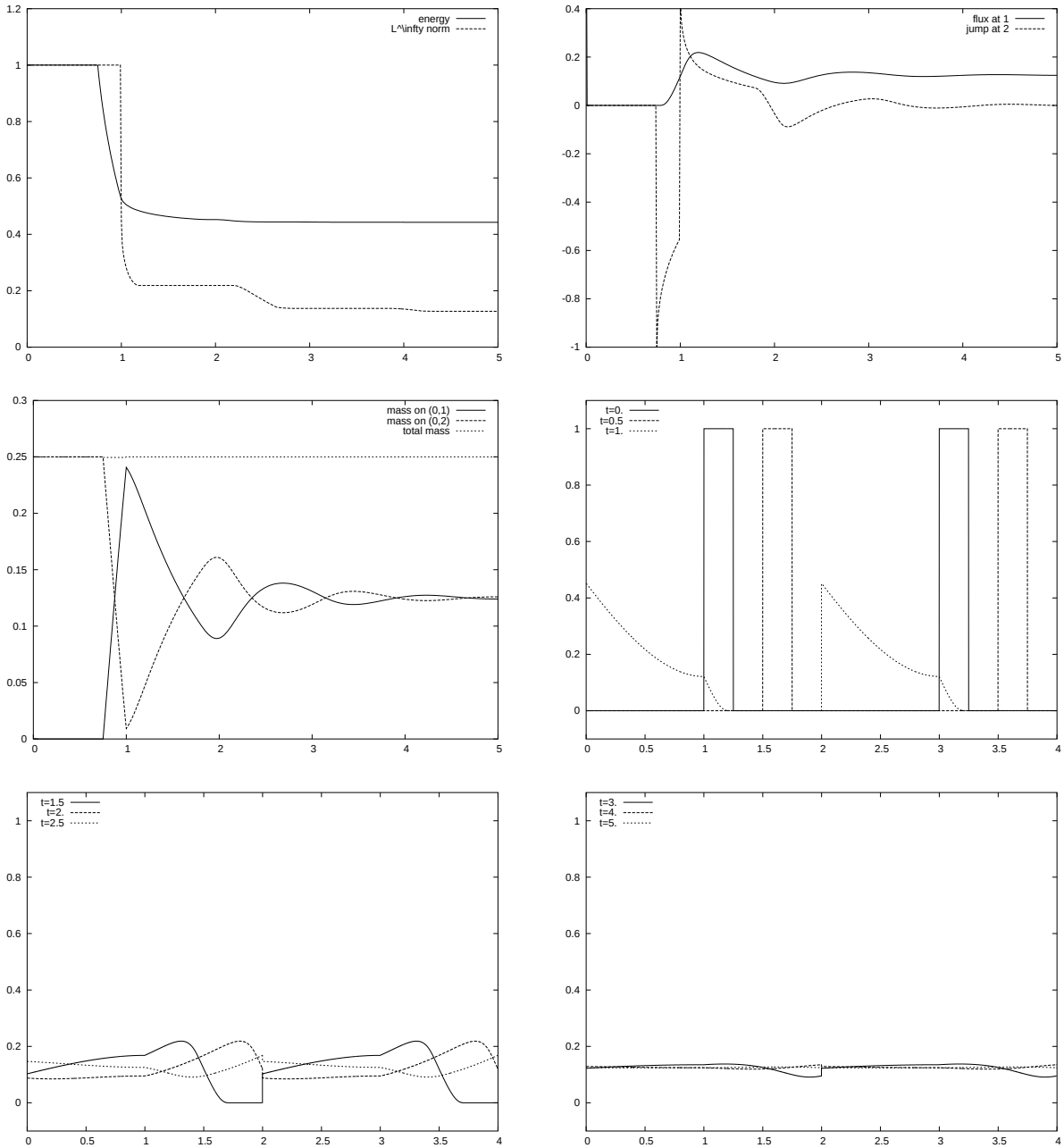

Figure 4. Reference solution for case 3: $\alpha = 1.$ and $u_0(x) = 1_{\{x\in[1.;1.25]\}}$.

- The flux at $x = 1$ and the jump at $x = 2$, as a function of time.
- The masses $\int_0^1 u$, $\int_1^2 u$, and $\int_0^2 u$ as a function of time. Owing to the periodicity of the flux, the total mass is conserved in time (since $f = 0$).
- The profiles $x \mapsto u(t,x)$ (represented on $(0,4)$ to illustrate periodicity) at times $t = 0$, 0.5, 1, 1.5, 2, 2.5, 3, 4, and 5.

For case 1 where the initial data is smooth (see Figure 2), the amount of energy dissipation is small. The homogeneous Neumann condition at 1^- and the jump at $2^-/0^+$ are clearly visible. This jump (which is initially zero) peaks in the time interval $t \in (1,2)$, i.e., after the initial data has reached the hyperbolic to parabolic interface.

For case 2 (see Figure 3), the jump at $2^-/0^+$ is discontinuous when the singularities in the initial data reach the interface, i.e., at times $t = 0.75$ and $t = 1$. The solution is in $D(A)$ for $t > 1$ in agreement with Proposition 2.1. The homogeneous Neumann condition at 1^- is again clearly visible. Similar conclusions can be drawn for case 3 (see Figure 4). An important difference is the larger amount of energy dissipation owing to the larger value of the diffusion coefficient. As a result, the second singularity in the jump is much smaller than for case 2 (peak value of 0.4 instead of 1).

Convergence tests are presented in Table 1 for case 1. The solution presented in Figure 2, say u_{ref}, is used as a reference to evaluate the errors associated with approximate solutions obtained on coarser grids and with larger time steps. Let $u_{h\delta t}$ be the approximate solution and let $e = u_{\text{ref}} - u_{h\delta t}$ be the error. For a function depending on time, say $v(t)$, we consider the discrete norms $\|v\|_{\ell^\infty(0,T)} = \max_{0 \leqslant n\delta t < T} |v(n\delta t)|$ and $\|v\|_{\ell^1(0,T)} = \frac{\delta t}{T} \sum_{0 \leqslant n\delta t < T} |v(n\delta t)|$. The results presented in Table 1 show that, as expected theoretically, the scheme is second-order in space and first-order in time for the three error measures.

		$\|e(t,\cdot)\|_{L^\infty(\Omega)}$		$\|\mathscr{F}(t,1)\|_{\ell^p(0,5)}$		$\|\mathscr{E}(t)\|_{\ell^p(0,5)}$	
h	δt	$t=1$	$t=5$	$p=\infty$	$p=1$	$p=\infty$	$p=1$
0.02	10^{-6}	1.1e-3	7.4e-4	1.1e-3	4.1e-4	1.6e-4	4.3e-5
0.01	10^{-6}	2.6e-4	1.8e-4	2.6e-4	1.0e-4	4.0e-5	1.1e-5
0.005	10^{-6}	6.4e-5	4.5e-5	6.4e-5	2.5e-5	1.0e-5	2.6e-6
0.02	2×10^{-5}	2.0e-4	1.8e-4	2.2e-4	9.8e-5	1.3e-4	9.3e-5
0.02	10^{-5}	9.3e-5	8.7e-5	1.0e-4	4.7e-5	6.0e-5	4.4e-5
0.02	5×10^{-6}	4.2e-5	3.9e-5	4.5e-5	2.1e-5	3.0e-5	2.0e-5

Table 1. Convergence analysis: h denotes the space step and δt the time step.

4. RESULTS WITH GLOBAL SCHEMES

This section presents results obtained with schemes in which the continuity of the solution at the parabolic to hyperbolic interface is not enforced explicitly. We consider an upwind scheme, a finite volume box-scheme introduced in [5,7], and a local discontinuous Galerkin method derived in [4].

4.1. Upwind scheme

To illustrate the numerical results that can be obtained for the evolution problem (1.3)–(1.4)–(1.5) with a very simple scheme, we consider a continuous piecewise-linear finite element method on $(0,2)$ with periodic conditions on the solution and with first-order artificial viscosity in the hyperbolic subdomain Ω_H. The mesh is uniform with step size h, and the artificial viscosity is set to $\varepsilon = \frac{h}{2}$. The scheme is equivalent to discretizing the spatial derivatives with centered differences in Ω_P and an upwind scheme in Ω_H. In both subdomains, time integration is performed using an implicit Euler method without lumping of the mass matrix. The time step is set to $\delta t = 10^{-4}$. Two meshes of Ω are considered, one with 200 cells and one with 400 cells. The corresponding solutions are termed the "coarse grid/upwind" solution and the "fine grid/upwind solution."

Results are presented in Figure 5. For the sake of brevity, we only show the time evolution of the normalized energy, the $L^\infty(\Omega)$-norm of the solution, the flux at $x = 1$, and the jump at $2^-/0^+$ estimated by the difference $u(t,2) - u(t,2-h)$. To facilitate comparisons with the reference solutions, these quantities are plotted using the same scale as in the two upper panels of Figures 2–4. In all cases, the correct physical behavior is recovered, confirming that the vanishing viscosity solution can capture the physically relevant interface condition. For case 1 where the initial data is smooth, the coarse grid/upwind solution, the fine grid/upwind solution, and the reference solution agree well. Minor discrepancies between coarse and fine grid solutions are observed in the energy profile. The situation is different for case 2 where the initial data is rough. Owing to the high level of dissipation induced by the scheme, significant errors are observed in the energy and jump profiles even on the fine grid/upwind solution. The singularities in the jump as the leading and trailing edges of the initial condition leave the hyperbolic subdomain are clearly under-resolved. Moreover, the asymptotic value of the energy (at time $t = 5$) is underestimated by 28.1% with the coarse grid/upwind solution and by 19.9% with the fine grid/upwind solution. The same conclusions hold for case 3 although the diffusion coefficient is larger.

4.2. Box-scheme

The box-scheme that we use to simulate the evolution problem is a high order box-scheme introduced in [5,7]. Box-schemes, like the Preissmann scheme, are commonly used in surface flow simulations (e.g., river flows, dam breaking) as well as in groundwater flow simulations (e.g., sedimentation, pollutant transport); see [10].

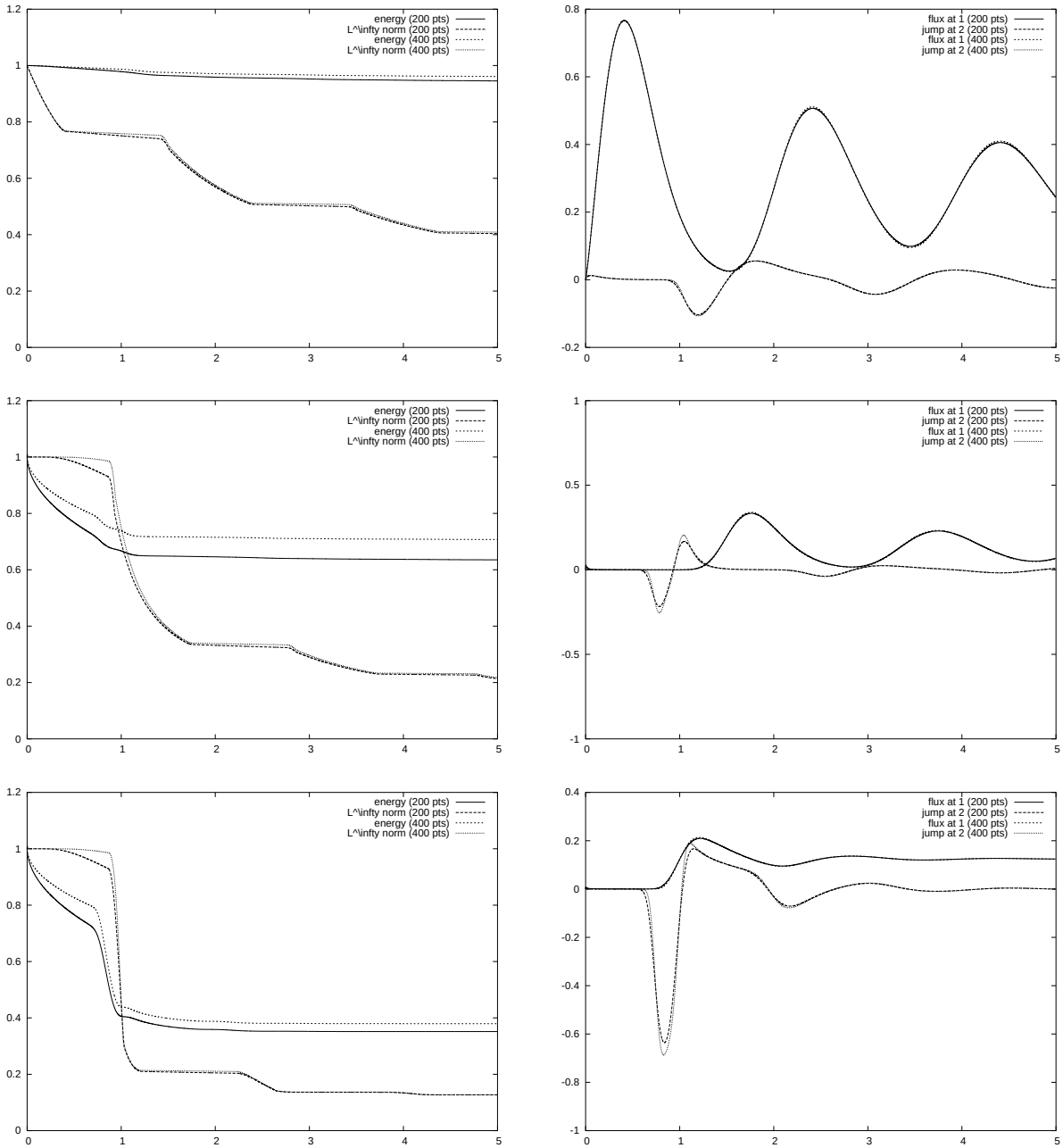

Figure 5. Numerical results obtained with the upwind method: case 1 (top), case 2 (center), and case 3 (bottom). Left panels: normalized energy and $L^\infty(\Omega)$-norm of the solution; right panels: the flux at $x = 1$ and the jump at $2^-/0^+$.

We shortly present the main features of our box-scheme. First, equation (1.3) is recast in mixed form using the diffusive flux $p(x) = -\alpha(x)u_x$ as an auxiliary unknown. This yields

$$\begin{cases} \partial_t u + \partial_x(u+p) = f & (t,x) \in [0,\infty) \times (0,2), \\ p = -\alpha(x)\,\partial_x u & (t,x) \in [0,\infty) \times (0,2), \\ (u+p)(t,0) = (u+p)(t,2), & t \in [0,\infty), \\ u(0,x) = u_0,\ p(0,x) = -\alpha(x)\,u_0'(x) & x \in (0,2). \end{cases} \tag{4.1}$$

Let $\mathscr{M} = \cup_{j=1}^{N}[x_j, x_{j+1}]$ be a mesh of Ω, δt be the time step, and set $t^n = n\delta t$. Set $h_{j-1/2} = x_j - x_{j-1}$ and introduce the box $K_{j-1/2} = [x_{j-1}, x_j]$ for $2 \leqslant j \leqslant N+1$. We assume that the mesh is compatible with the partitioning of Ω into Ω_P and Ω_H so that α is constant on each box; let $\alpha_{j-1/2} = \alpha_{|K_{j-1/2}}$. Taking the mean value of the first two equations in (4.1) on a box yields the two following identities verified by the *exact solution*:

$$h_{j-1/2}\,\frac{\mathrm{d}}{\mathrm{d}t}(\Pi^0 u)_{|j-1/2}(t) + [\mathscr{F}(x_j,t) - \mathscr{F}(x_{j-1},t)] = h_{j-1/2}\,(\Pi^0 f)_{|j-1/2}(t), \tag{4.2}$$

$$h_{j-1/2}\,(\Pi^0 p)_{|j-1/2}(t) = -\alpha_{j-1/2}\,[u(x_j,t) - u(x_{j-1},t)], \tag{4.3}$$

where Π^0 denotes the averaging operator on the boxes and $\mathscr{F}(x_j,t) = u(x_j,t) + p(x_j,t)$. The box-scheme evolves simultaneously 3 quantities:

- The values u_j^n and p_j^n at the points of the mesh; these values are such that $u_j^n \simeq u(x_j,t^n)$ and $p_j^n \simeq p(x_j,t^n) = -\alpha(x_j)u_x(x_j,t^n)$.
- The mean-value $\overline{u}_{j-1/2}$ in each box $K_{j-1/2}$ such that $\overline{u}_{j-1/2} \simeq (\Pi^0 u)_{|j-1/2}(t^n)$.

Using a ϑ-scheme for the time integration of (4.2) yields

$$\delta\overline{u}_{j-1/2}^n = -\tfrac{1}{h_{j-1/2}}(F_j^n - F_{j-1}^n) - \tfrac{\vartheta\delta t}{h_{j-1/2}}\,(\delta u_j^n + \delta p_j^n - \delta u_{j-1}^n - \delta p_{j-1}^n) + \mathscr{R}_{j-1/2}^n(f), \tag{4.4}$$

with $F_j^n = u_j^n + p_j^n$ and $\mathscr{R}_{j-1/2}^n(f) = (1-\vartheta)(\Pi^0 f)_{|j-1/2}(t^n) + \vartheta\,(\Pi^0 f)_{|j-1/2}(t^{n+1})$. In addition, we have introduced the discrete time derivative operator δ such that for a time discrete sequence $(Z^n)_{n\geqslant 0}$, $\delta Z^n = \frac{Z^{n+1}-Z^n}{\delta t}$. The relation (4.4) only contains the parameter ϑ selected for the time scheme.

The second relation used in the box-scheme expresses the link between the incremental value of $\delta\overline{u}_{j-1/2}^n$ and the two values δu_j^n and δu_{j-1}^n. It can be seen as a *local model* at the scale of the box. We use a model with 3 parameters consisting of a relaxation scheme in the form

$$\begin{aligned} \left(\frac{1}{2} + D_{U,j-1/2}^n\right)\,\delta u_j^n + \left(\frac{1}{2} - D_{U,j-1/2}^n\right)\,\delta u_{j-1}^n - \delta\overline{u}_{j-1/2}^n = \\ -\frac{\zeta_{j-1/2}^n}{\delta t}\,(M_{E,j-1/2}^n - \overline{u}_{j-1/2}^n), \end{aligned} \tag{4.5}$$

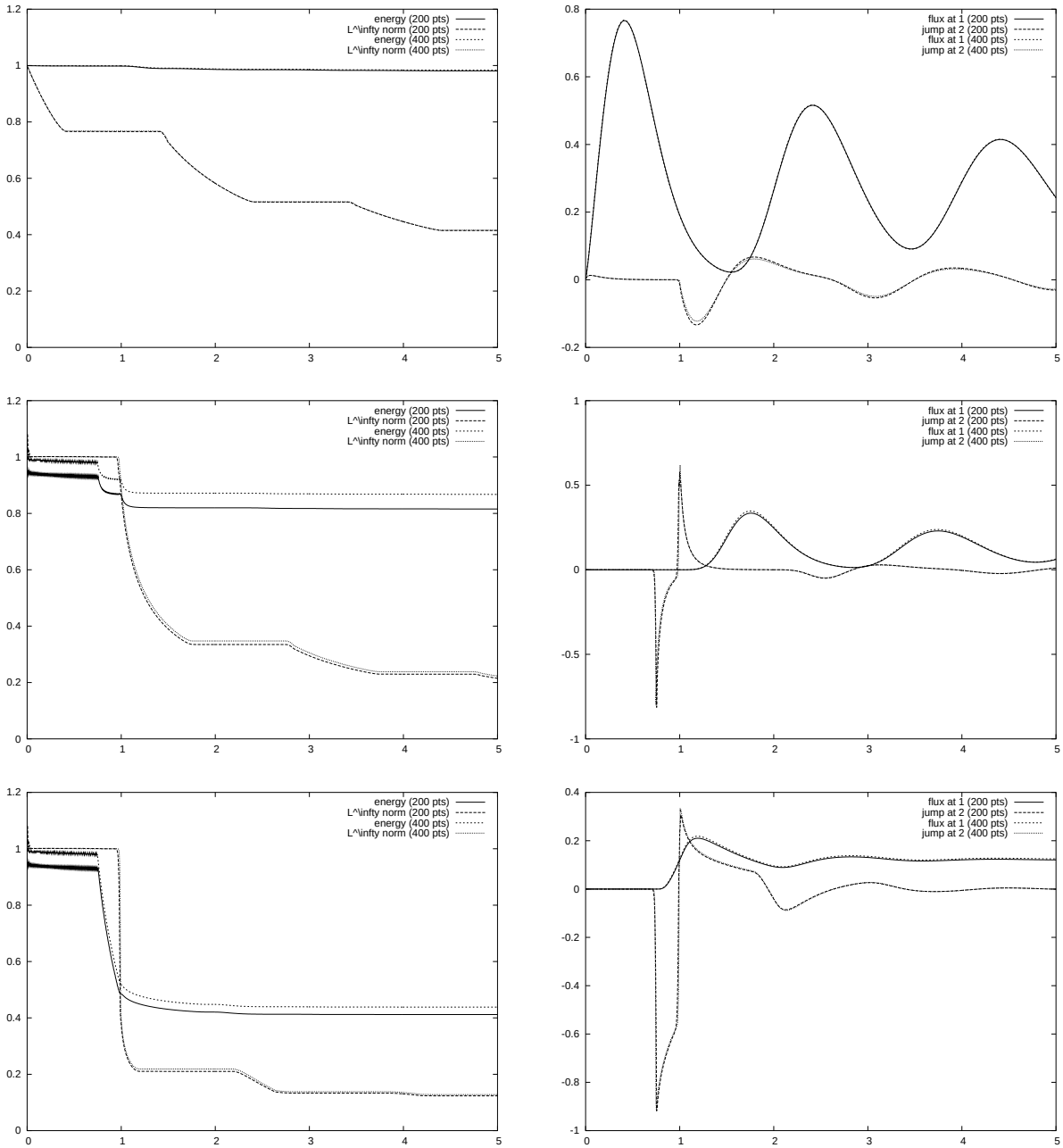

Figure 6. Numerical results obtained with the box-scheme: case 1 (top), case 2 (center), and case 3 (bottom). Left panels: normalized energy and $L^\infty(\Omega)$-norm of the solution; right panels: the flux at $x = 1$ and the jump at $2^-/0^+$.

where $M^n_{E,j-1/2}(u)$ stands for an *equilibrium average value* defined by

$$M^n_{E,j-1/2}(u) = \left(\frac{1}{2} + D^n_{E,j-1/2}\right) u^n_j + \left(\frac{1}{2} - D^n_{E,j-1/2}\right) u^n_{j-1}. \tag{4.6}$$

Finally, we need a local model for (4.3) expressing the closure law for the diffusive flux p. We use an upwinded quadrature formula to approximate $(\Pi^0 p)_{|j-1/2}(t^n)$ by the quantity

$$\overline{p}^n_{j-1/2} = \frac{1}{2}[p^n_j + p^n_{j-1}] - D_{p,j-1/2}[p^n_j - p^n_{j-1}]. \tag{4.7}$$

Equations (4.5) and (4.7) contain 4 parameters in each box $K_{j-1/2}$ at each time t^n, which have to be specified: the two upwind parameters, $D_{U,j-1/2}$ and $D_{E,j-1/2}$ in (4.5) and (4.6), respectively; a time parameter $\zeta_{j-1/2}$ to define the relaxation time scale $\delta t/\zeta_{j-1/2}$ in (4.5); and the parameter $D_{p,j-1/2}$ to define the averaged diffusive flux p in (4.7). The values taken by these four parameters rely on the numerical analysis presented in [5,6,7]. It consists, on the one hand, of a time-independent analysis, allowing to select D_p in a way ensuring a non-oscillating stationary state for the convection-diffusion equation [6]; on the other hand, of a time-dependent analysis based on the notion of *equivalent equation* [5,7]. This allows to define the three parameters D_U, D_E, and ζ to achieve a high-order accuracy. The present box-scheme can be expressed as a 3-point implicit scheme in the incremental values δu^n_j. Finally, we stress the fact that the box-scheme is used in both the parabolic and the hyperbolic subdomains. It has been proved to be accurate in all Peclet regimes.

Results with equispaced meshes of 200 and 400 boxes are displayed in Figure 6. In all computations, the time step is selected according to a CFL number of $\frac{\delta t}{h} = 0.5$. The accuracy of the scheme can be observed on the low energy dissipation and on the sharp resolution of the jump at $x = 2$. For instance, at time $t = 5$ and for case 2, the value of the energy is underestimated by 7.6% on the coarse grid and by 1.7% on the fine grid, a significant improvement with respect to the upwind scheme.

4.3. Local Discontinuous Galerkin (LDG)

The local discontinuous Galerkin method was developed by Cockburn and Shu [4] for convection-diffusion equations based on earlier work devoted to hyperbolic conservation laws. A complete review of the LDG method and other discontinuous Galerkin methods can be found in [3] and references therein.

As for the finite volume box-scheme, let $\mathscr{M} = \cup_{j=1}^N K_{j+1/2}$ be a mesh of Ω and assume that the mesh is compatible with the partitioning of Ω into Ω_P and Ω_H. Let k be a positive integer. Let V^{DG} be the space of piecewise discontinuous functions in Ω that are polynomials of degree $\leqslant k$ in each cell $K_{j+1/2}$ for $1 \leqslant j \leqslant N$. Let V^{DG}_P be the subspace of V^{DG} spanned by those functions that vanish identically on Ω_H. For a function $v_h \in V^{\mathrm{DG}}$, we denote its left and right traces at a point x_j in the mesh as

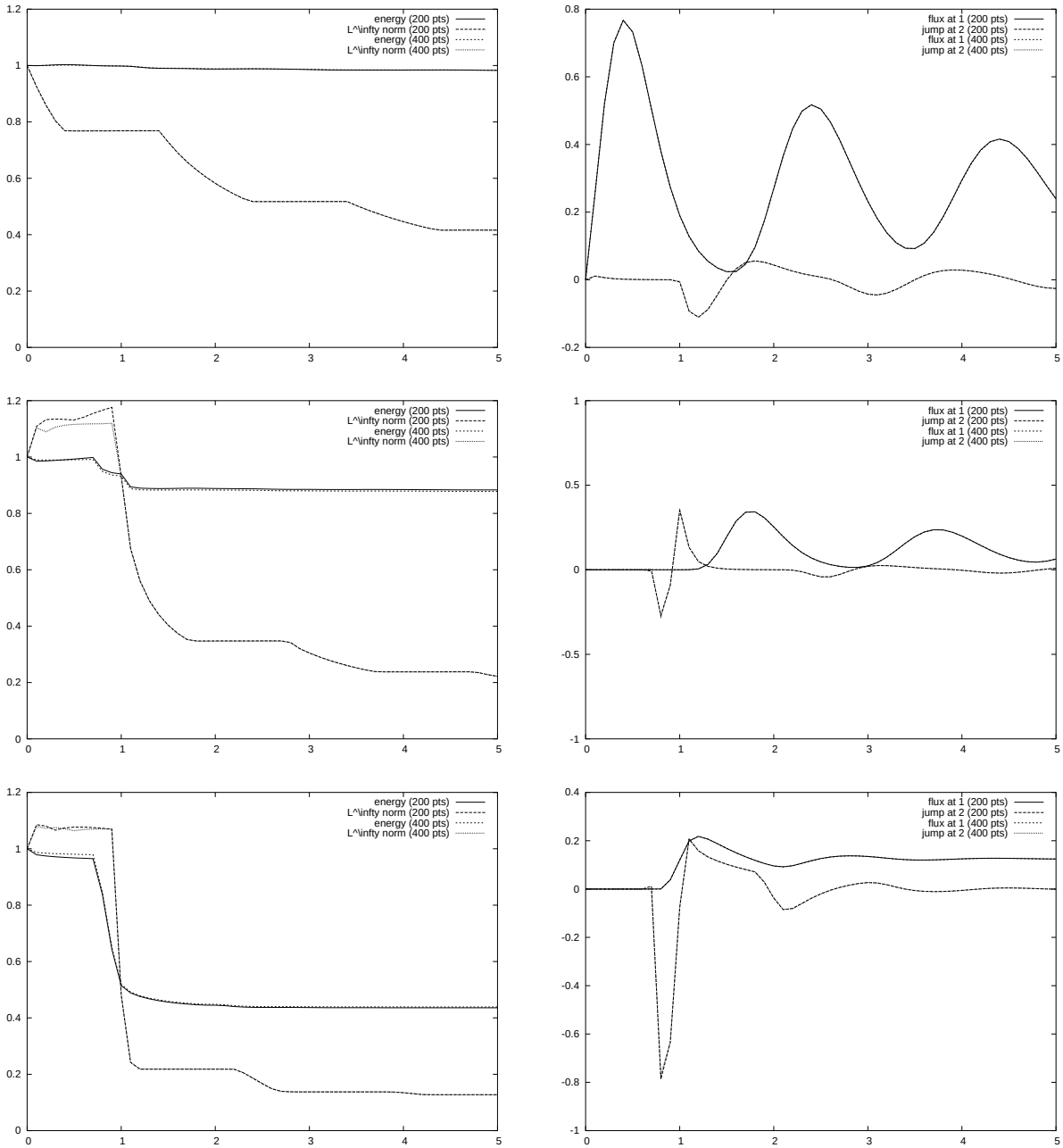

Figure 7. Numerical results obtained with the LDG method: case 1 (top), case 2 (center), and case 3 (bottom). Left panels: normalized energy and $L^\infty(\Omega)$-norm of the solution; right panels: the flux at $x = 1$ and the jump at $2^-/0^+$.

$v_h^{\pm}(x_j) = \lim_{s\to 0^+} v_h(x_j \pm s)$, $1 \leqslant j \leqslant N$, and we define its jump and average across inner element boundaries as

$$[v_h(x_j)] = v_h^+(x_j) - v_h^-(x_j) \quad \text{and} \quad \{v_h(x_j)\} = \tfrac{1}{2}(v_h^+(x_j) + v_h^-(x_j)), \quad 1 \leqslant j \leqslant N.$$

The LDG method consists of seeking $u_h \in C^1([0,\infty[;V^{\mathrm{DG}})$ such that, for all $v_h \in V^{\mathrm{DG}}$ and $t \geqslant 0$,

$$\begin{aligned} \frac{\mathrm{d}}{\mathrm{d}t}(u_h, v_h)_\Omega - \sum_{j=1}^{N} (u_h + z_h, v_{h,x})_{K_{j+1/2}} - \sum_{x_j \in \Omega} u_h^-(x_j)\,[v_h(x_j)] \\ - \sum_{x_j \in \Omega_P} \{z_h(x_j)\}[v_h(x_j)] - z_h^-(1)[v_h(1)] = (f, v_h)_\Omega, \end{aligned} \tag{4.8}$$

and $z_h \in C^0([0,\infty[;V_P^{\mathrm{DG}})$ such that, for all $v_h \in V_P^{\mathrm{DG}}$ and $t \geqslant 0$,

$$\begin{aligned} (z_h, w_h)_\Omega - \sum_{j=1}^{N} \alpha_0 (u_h, w_{h,x})_{K_{j+1/2}} - \sum_{x_j \in \Omega_P} \alpha_0 \{u_h(x_j)\}\,[w_h(x_j)] \\ + \alpha_0 \left((u_h w_h)(1^-) - (u_h w_h)(0^+) \right) = 0. \end{aligned} \tag{4.9}$$

Note that (4.9) is a local reconstruction formula for the diffusive flux in Ω_P, while (4.8) is the discretization of the evolution equation using the reconstructed flux. As for the finite volume box-scheme, the continuity of the solution at $x = 1$ is not used. The periodicity of the flux is weakly enforced in (4.8). Finally, Problem (4.8)–(4.9) is discretized in time via a simple explicit Euler method (without slope limiting).

Results are presented in Figure 7. Two uniform meshes of Ω are considered: a coarse mesh with 200 cells and a fine mesh with 400 cells. The time step is obtained from the diffusive stability limit $\delta t = \frac{1}{10}\frac{h^2}{\alpha_0}$. For case 1 where the initial data is smooth, excellent agreement is obtained. For cases 2 and 3 where the initial data is rough, the Gibbs phenomenon is triggered causing the $L^\infty(\Omega)$-norm of the solution to be larger than 1 until the singularities have left the hyperbolic subdomain. This phenomenon can be cured by a suitable slope limiter, but this is not the scope of the present work. We also observe that the jump at $2^-/0^+$ is captured with slightly less accuracy than the box-scheme. At time $t = 5$ and for case 2, the value of the energy is underestimated by 2.9% on the coarse grid and by 1.2% on the fine grid, yielding a slightly better accuracy than the box-scheme.

5. CONCLUDING REMARKS

In this paper, we have analyzed a degenerate one-dimensional advection-diffusion equation with periodic interface conditions for the total advective-diffusive flux. Using the evolution linear semi-groups theory, we have shown that the associated Cauchy problem is well-posed provided it is supplemented with an additional continuity condition on the solution at the parabolic to hyperbolic interface. Reference

solutions have been obtained for various sets of data (initial condition, diffusion coefficient) and can now be used by practitioners to test the robustness of numerical schemes to approximate flows in media with strong heterogeneities.

To conclude, we point out that various interesting theoretical points have been postponed to future work, including the convergence analysis of the various schemes presented above. Furthermore, a classical question to which it is often difficult to answer is to know in which sense the function $u(t) = T(t)u_0$ given by the semi-group theory solves the evolution problem when the initial condition is too rough to be in the domain of the evolution operator. Although we have constructed a weak solution to the evolution problem for a rather general class of initial conditions, it is not yet clear that these solutions are those given by the semi-group theory. Periodic distributions and Fourier series techniques could be used to tackle this question.

Acknowledgments. The authors are grateful to E. Cancès, R. Eymard, and R. Monneau for fruitful discussions.

REFERENCES

1. H. Brezis, *Analyse fonctionnelle*. Masson, Paris, 1987.
2. T. Cazenave and A. Haraux, *Introduction aux problèmes d'évolution semi-linéaires*. Ellipses, Paris, 1990.
3. B. Cockburn, G. Karniadakis, and C. Shu, The development of discontinuous Galerkin methods. In *Discontinuous Galerkin Methods* (Eds. B.Cockburn, G.Karniadakis, and C.Shu). Springer-Verlag, Berlin, 2000.
4. B. Cockburn and C.-W. Shu, The local discontinuous Galerkin method for time-dependent convection-diffusion systems, *SIAM J. Numer. Anal.* (1998) **35**, 2440–2463.
5. B. Courbet, Etude d'une famille de schémas boite `a deux points et application `a la dynamique des gaz monodimensionnelle. *La Recherche Aérospatiale* (1991) **5**, 31-44.
6. J-P. Croisille, Keller's box-scheme for the one-dimensional stationary convection-diffusion equation. *Computing* (2002) **68**, 37–63.
7. J-P. Croisille, A high order accurate box-scheme for the one dimensional convection-diffusion equation. Preprint, Metz University (2002).
8. J.-P. Croisille and I. Greff, An efficient box-scheme for convection-diffusion equations with sharp contrasts in the diffusion coefficient. To appear in *Comput. Fluids* (2004).
9. F. Gastaldi and A. Quarteroni, On the coupling of hyperbolic and parabolic systems: Analytical and numerical approach. *Appl. Num. Math.* (1989) **6**, 3–31.
10. F.M. Holly and A. Preissmann, Accurate calculation of the transport in two dimensions. *Journal of Hydraulics Division* (1977) 1259–1277.
11. J.-L. Lions, *Quelques méthodes de résolution des problèmes aux limites non linéaires*. Dunod, Paris, 1969.
12. A. Pazy, *Semigroups of Linear Operators and Applications to Partial Differential Equations*. Springer, New York, 1983.
13. A. Quarteroni and A. Valli, *Numerical Approximation of Partial Differential Equations*. Springer, Berlin, 1997.